ELSEVIER

Journal of Nuclear Materials 241–243 (1997) 260–267

journal of nuclear materials

# The influence of key operation parameters and material properties on the quantification of tritium inventory and permeation in the plasma facing components of ITER

G. Federici [a,*], D. Holland [b], G. Janeschitz [a], C.H. Wu [c]

[a] *ITER JWS Garching Co-center, Boltzmannstraße 2, 85748 Garching, Germany*
[b] *ITER JWS Naka Co-center, 801-1 Mukouyama, Naka-machi, Naka-gun, Japan*
[c] *The NET Team, Boltzmannstraße 2, 85748 Garching, Germany*

**Abstract**

This paper identifies the relevant uncertainty parameters affecting the tritium inventory and permeation estimates for three candidate ITER plasma facing materials (i.e., Be, presently the only material under consideration for the first wall and start-up limiter; Be and W for the baffle; and Be, W, and CFC for the divertor). An analysis was conducted to quantify the changes of the tritium inventory and permeation resulting from the varying parameters with the highest uncertainty. It includes the effects of plasma physics parameters (i.e., heat and particle fluxes, net-erosion rate), material properties (i.e., diffusion coefficient, rate of surface recombination and the possible presence of surface oxide layers), nuclear radiation (i.e., density of $n$-induced traps), design and operational lifetime (i.e., type and thickness of plasma facing components materials and replacement schedule for the sacrificial components exposed to high particle and heat fluxes). Based on the results, the implications on the design are discussed and priorities are determined for the R&D needed to reduce the uncertainties.

*Keywords:* ITER; Wall particle retention; Tritium inventory and economy; Fusion technology

## 1. Introduction / background

Despite a considerable amount of new experimental information, available both from operational experience in existing tokamaks and from laboratory studies, and the remarkable modelling progress which has taken place during the past decade, there are still large uncertainties in quantifying tritium inventory in- and permeation through plasma facing materials (PFM's) in the International Thermonuclear Experimental Reactor (ITER). Estimation of this uncertainty is indispensable to an understanding of the radiological hazards from tritium permeation into coolants and from potential accidents, as well as for the assessment of the fuelling requirements. In addition, these estimates contribute to the decisions involving the choice of different armor material options.

This study builds on estimates of tritium inventory and permeation reported in Ref. [1] and identifies all the relevant parameters governing or affecting the accumulation of tritium in the in-vessel components of ITER during the so-called 'basic-performance-phase' (BPP). An analysis was conducted to estimate the changes of the inventory and of the permeation resulting from varying some of the key parameters subject to the largest uncertainty in the ranges of interest and the resulting implications on the design are discussed.

The mobile and trapped inventory as well as the permeation rate and breakthrough time were calculated using the simplified model described in Refs. [2,3] that combines the effects of erosion with tritium dynamics at surfaces and in bulk materials. The physics foundation of the model and the governing equations are described in detail in Ref. [2]. In this model, the atoms implanted in the near-surface

* Corresponding author. Tel.: +49-89 3299 4228; fax: +49-89 3299 4110; e-mail: federig@itereu.de.


*PII* S0022-3115(96)00511-9

layer diffuse in the bulk and they are trapped as they encounter empty trap sites. Trapping and detrapping are assumed to occur much faster than diffusion of mobile tritium atoms. Consequently, there would be a moving front in the material behind which all traps are filled and ahead of which all traps are empty. The mobile concentration would then be zero ahead of the front. Behind the front, the concentration would vary from the near-surface concentration value, $C_0$, at the face to zero at the location of the moving front. Also, the effects of erosion which takes place simultaneously with implantation, e.g., reduction of the amour thickness, removal of the tritium mobile and trapped in the eroded layer, reduction of the surface temperature and change of the temperature gradient, etc., are accounted for in this model. The change of the tritium uptake properties, which is still uncertain, resulting from microdamage formation in the near surface due to implantation/erosion mechanisms is not included.

## 2. Sources of uncertainty

Table 1 taken from Ref. [4] shows the uncertainty parameters.

The parameters considered in this study are:

### 2.1. Materials

Beryllium is the main material under consideration for the first wall, start-up limiter and the upper portion of the baffle (see Fig. 1). However, because of its favorable behaviour under high heat flux, carbon fibre composites (CFC's) could also be used for protecting the baffle and the limiter, but were not considered in this study. Tungsten and beryllium are being considered for the lower portion

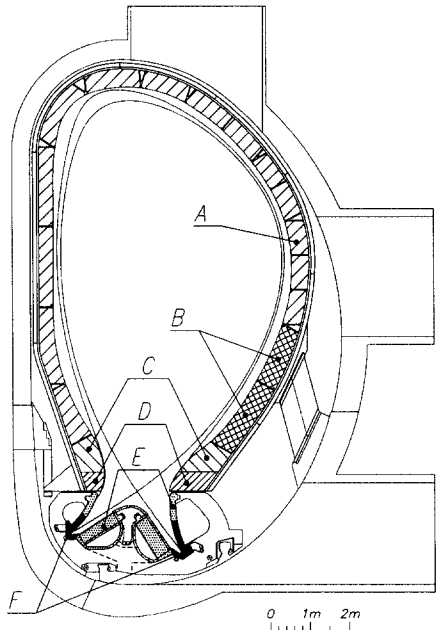


Fig. 1. Schematic layout of the PFC's in ITER. (Symbols – A: first wall, B: limiter, C: upper-baffle, D: lower-baffle, E: divertor (low flux region), F: divertor (high flux region.)

Table 1
Parameters important for tritium inventory or permeation in ITER-plasma facing components (PFC's)

| Parameters | Uncertainty | Importance inventory | Importance permeation | Selected in this study |
|---|---|---|---|---|
| 1. Materials used in PFCs | H | H | H | yes |
| 2. Materials used for substrate | L | L | L | no |
| 3. Particle flux and energy | H | H | H | yes |
| 4. Heat flux or temperature | H | H | H | yes |
| 5. Affected area | H | H | M | see Ref. [4] |
| 6. Thickness of PFC materials | H | H | H | yes |
| 7. Thickness at end-of-life | H | L | M | yes |
| 8. Codeposition rates | H | H | L | no [b] |
| 9. Erosion removal rate | H | M | H | yes |
| 10. Trap density and energy | H | H | H | yes |
| 11. Trap production schedule | H | L | M | no |
| 12. Recombination coefficient | H | H | H | yes |
| 13. Diffusion rate | H [a] | H | H | yes |
| 14. Solubility | H | L | L | no |
| 15. Oxide layer blocking implantation | H | H | H | yes |
| 16. Replacement schedule | H | M | H | yes |
| 17. Baking temperature and schedule | H | L | M | no |
| 18. Implantation depth | L | M | M | no |
| 19. Breeding rate from neutrons | L | L | L | no |

H = high, M = moderate, L = low.
[a] For Be only.
[b] See Refs. [1,5].

of the baffle while for the divertor, tungsten and CFC's are presently being considered as primary candidates.

### 2.2. Particle flux

The particle flux and the energy distribution on the various components are difficult to estimate for ITER conditions. In general a factor of 10 up or down was used for the uncertainty. However, the upper implantation rate was limited to $10^{23}$ DT/m$^2$/s since high fluxes occur with low energy which results in a high reflection coefficient [6].

### 2.3. Heat flux

For the first wall and divertor components with low heat flux, higher heat fluxes ($\sim$ twice the peak design value) were investigated. For the lower baffle and divertor components with high heat flux, lower heat fluxes ($\sim$ half of the peak design value) were investigated (see Table 2).

### 2.4. Thickness of PFM's

The effect of varying the thickness was investigated for the various materials and the range is indicated in Table 2. Probably, armors thinner than 5 mm might not be used, even on the primary first wall where, in spite of the much lower erosion rate, thick Be armors are deemed to be necessary to inertially counteract the thermal propagation of large heat loads resulting from abnormal operation which can bring the plasma in contact with the wall, e.g., during vertical displacement events (see Ref. [7] and references therein).

### 2.5. Erosion removal rate

For the first wall, little erosion is expected. Rates of up to 1 nm/s were considered. For the high-flux components, rates from 0.1 to 3 nm/s were considered for the case of beryllium and from 0.01 to 1 nm/s for the case of tungsten.

### 2.6. Trap density

The density and binding energy of traps depend on material, fabrication, and radiation exposure. Densities could range from 0.01 to 0.1 at%. Traps binding energy assumed in the calculations are similar to those available in the literature, i.e., 1.8 eV for Be, 1.5 eV for W and 4.3 eV for C.

### 2.7. Recombination coefficient

Recombination for beryllium is highly uncertain strongly influenced by the material and surface conditions, with clean surfaces giving the highest recombination. To account for this uncertainty we bracketed the value recommended by experts (see Ref. [8]) up and down by a factor of 10. Even though preliminary and awaiting further experimental confirmation, some new experimental results on tritium implantation in beryllium are becoming available [9] and contrary to the original expectation, recombinative desorption of implanted hydrogen ions at least at high fluxes seems to be largely enhanced due to the increase of the exchange surface area resulting from substantial micro damage. This in turn could result in much higher recombination coefficients that those indicated in Refs. [8,10] which provided the basis for the values assumed in this study. However, exposure to lower particle and heat fluxes (representative of the first wall of ITER), in addition to effects resulting from mixing of materials and the contamination of the Be surfaces with C and O remain still to be carefully investigated.

### 2.8. Diffusion rate

The diffusion rate is fairly well known for PFM's like tungsten and graphite, less for CFC's and Be. Because of the small amount of CFC used in our design and the relatively low operating bulk temperatures, the contribution to the inventory deriving from diffusion of tritium in the bulk of this material is neglected. Since $K_R$ was determined for beryllium by measurements of $D/K_R$ [8], when we changed $D$ for beryllium, to be consistent, we also changed $K_R$. However, since other factors such as surface condition influence $K_R$, $D$ was not adjusted when $K_R$ was varied.

### 2.9. Oxide layer blocking implantation

Residual oxygen in the torus may oxidise beryllium surfaces at a faster rate than removal by ion sputtering. There is evidence of oxide layers forming at or just below the surface. Oxide layers have been determined to be barriers to permeation. Based on parameters estimated for ITER, this situation could hold for the first wall, upper baffle, start-up limiter, and the low flux portion of the divertor, but is not likely for the high flux components. Where this oxide layer was assumed to be present in the parameter study, the inventory in that component was considered to be zero.

### 2.10. Replacement schedule

The first wall and start-up limiters are designed as lifetime components. The baffle is exposed to higher fluxes and may require replacement. The divertor is expected to be replaced 3 times during the BPP. Two cases were considered to bracket replacement schedule. In both cases, no replacement of the first wall, limiter, or baffle was considered.

- Base case—All divertor components are at breakthrough or end of life (EOL), whichever comes first.

- Alternate case—More frequent replacement result in half the divertor cassettes near the beginning of life (BOL) (no inventory or permeation) and half just after breakthrough or EOL, whichever comes first.

## 3. Cases analyzed

Fig. 1 shows the layout of the various ITER PFC's. Table 2 summarizes the ranges considered for the analysis. To simplify the analysis, PFC's with similar operational conditions are combined. Thus, the model for the first wall (FW) also includes the start-up limiter (SL) and the upper portion of the baffle (UB). The divertor components are separated into high (DHF) and low (DLF) heat flux operation. It is here assumed that about 50 $m^2$ of the divertor is subject to a heat flux of about 4 $MW/m^2$ and 150 $m^2$ of divertor area to a heat flux of about 1 $MW/m^2$. Additional details on the assumptions can be found in [4], while tritium transport material properties used for the various materials are reported in Ref. [2].

Although not included for detailed analysis here, two additional sources of tritium inventory were considered as well. The first is codeposition of T with eroded C or C/Be which forms a T-rich C-amorphous layer on redeposition-dominated surfaces of the PFC's. This occurs with no saturation limit and, therefore, its safety and operational implications are important. The second is the tritium generated by neutron transmutation in beryllium.

Tritium codeposition on the divertor and adjacent surfaces is being studied in detail in connection with overall erosion and lifetime analysis [1,5]. As discussed in Ref. [1], one to several kg T can be retained in the codeposited layers of ITER, unless effective conditioning techniques, yet to be developed, are applied. However, because of safety and tritium supply concerns, our study assumes the codeposited inventory to be mobilisable and limited to 1 kg T, implying that an efficient clean-up method, needs to be used every time this value is exceeded.

It is assumed in this study that the high neutron fluence at the first wall will result in breeding of about 200 g T by the end of the BPP [1]. This tritium is expected to migrate into sites, either traps or bubbles with relatively high binding energy and is therefore considered trapped.

## 4. Discussion of results

Calculations are performed for the reference case and for the end points of the parameter ranges summarized in Table 2. Results are displayed in scatter plots to help visualise the distribution.

### 4.1. Tritium inventory

The total (all PFC's) mobile and trapped inventory was calculated for the three following cases:

Case (1) design baseline armour material option [11]: which consists of Be on the FW/SL/UB, tungsten on the LB and on the DLF with the exception of a small portion DHF protected with CFC where disruptions and power excursions are expected to take place frequently; case (2)

Table 2
Ranges for parameters selected for the detailed analysis

| Area ($m^2$)/region in Fig. 1 | FW/SL/UB 1200/A [a] | LB 50/D | DLF 150/E | DHF 50/F |
|---|---|---|---|---|
| Particle flux ($DT/m^2/s$) | $10^{20}$ [b]–$10^{21}$ | $10^{21}$–$10^{23}$ [b] | $10^{21}$–$10^{23}$ | $10^{21}$–$10^{23}$ [b] |
| Heat flux (multiplying factor, see [b]) | 1–2 | 0.5–1 | 1–2 | 0.5–1 |
| Materials proposed in PFCs and thickness (mm) | Be 2–10 [b] | Be 5–10<br>W 5–10 [b] | Be 5–10<br>W 5–10 [b]<br>CFC 30 | Be 2–10<br>W 5–10<br>CFC 30 [b] |
| Erosion removal rate (nm/s) | | | | |
| Be | 0 [b] and 0.1–1 | 0.1–10 | 0.1–3 | 0.1–3 |
| W | — | 0.01–1 [b] | 0.01–1 [b] | 0.01–1 |
| Trap density (at%) | 0.01–1.0 | 0.01–1.0 | 0.01–1.0 | 0.01–1.0 |
| $D/2 \times K_R$ for beryllium (× [8]) | 0.1–10 | 0.1–10 | 0.1–10 | 0.1–10 |
| Recomb. coefficient, $K_R$ (× [8]) | 0.1–10 | 0.1–10 | 0.1–10 | 0.1–10 |
| Oxide layer blocking implantation | yes/no | no | yes/no | no |
| Replacement schedule (# in BPP) | 1 | 1-frequent | 3-frequent | 3-frequent |

[a] Region A = summation of regions A + B + C in Fig. 1.

[b] Reference baseline. Additional details for this case not indicated in the table are: (1) heat flux ($MW/m^2$): A [a] = 0.25, D = 3, E = 1, F = 4; (2) particle flux ($DT/m^2/s$): E = $10^{22}$; (3) temperature (°C) (plasma side/coolant side): A [a] = 225/165, D = 660/280[(i)], 590/280[(ii)], E = 290/175[(i)], 265/175[(ii)], F = 665/200[(i)], 760/200[(ii)], 800–1200/280[(iii)]; (4) trap density (at%) 0.1 for all materials. (superscripts: (i) Be, (ii) W, (iii) CFC.)

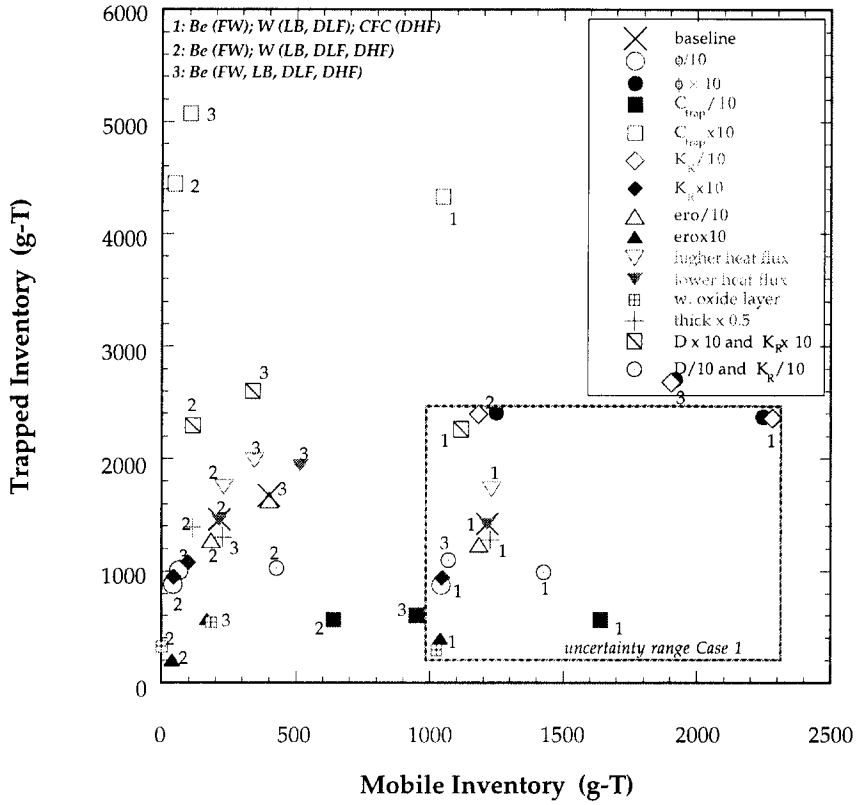


Fig. 2. Trapped inventory versus mobile inventory. Numbers in the figure refer to the various design options analyzed. (Abbreviations: FW = first wall, LB = lower baffle, DLF = low flux portion of divertor, DHF = high flux portion of divertor.)

which is the same as case (1) where CFC in the DHF is replaced with W; and case (3) which consists of an all Be machine, analysed here only for the sake of comparison. All cases included 200 g of trapped T in Be due to neutron transmutation. Case 1 includes 1000 g of mobile inventory due to codeposition.

The results for the inventory are plotted in Fig. 2 and for case (1) are summarised in Table 3. A rectangle was drawn on the plot to capture the ranges of uncertainty for the reference case 1. Extreme points that were higher than this range are further discussed below.

The analysis conducted shows that the variations of the parameters from the base values (see Table 2) that have the strongest implications on the design are: (i) increase of the particle flux, (ii) increase of the trap density, (ii) reduction of the recombination coefficient. As an example for case (1) an increase of the particle flux of a factor of 10 results in an increase of the mobile inventory from

Table 3
Summary of inventory ranges for case (1)

| Beryllium with tungsten lower baffle and divertor with some carbon | Mobile inventory (g T) | | | Trapped inventory (g T) | | |
|---|---|---|---|---|---|---|
| | baseline | low | high | baseline | low | high |
| First wall | 210 | 50 | 1150 | 1100 | 300 | 2000 |
| Bred tritium | | | | 200 | 200 | 200 |
| Lower baffle | 0.05 | 0.02 | 0.34 | 50 | 20 | 55 |
| LHF divertor | 0.2 | 0 | 7 | 45 | 10 | 140 |
| HHF divertor | 0.05 | 0 | 0.15 | 30 | 0 | 35 |
| Codeposited layers | 1000 | 1000 | 1000 | | | |
| Total | 1210 | 1050 | 2166 | 1425 | 530 | 2430 |

~ 1250 g to ~ 2250 g and of the trapped inventory from ~ 1500 g to ~ 2400 g (see Fig. 2). As explained in Refs. [2,3], the increase in mobile inventory results from two factors. The higher surface concentration causes higher bulk concentration since the bulk concentration varies approximately linearly from the surface concentration at the surface to zero at the trapping front. Also, the deeper penetration of the front creates a larger region for mobile tritium behind the front. The higher trapped inventory results from the deeper penetration of the front which increases the volume where trapping occurs. However, implanting flux this high in the divertor is not likely since baseline values are close to the upper values expected if reflection of low-energy particles is considered. In the first wall region, a factor of 10 higher flux of low energy particles it is only expected in a few localized positions near for instance the gas fuelling points. An other important parameter, particularly for beryllium, which has a strong bearing on the results is the value of the surface recombination coefficient. Decreasing recombination has a similar effect to increasing particle flux. The higher surface concentration leads to higher bulk concentrations. Also, the speed of the trapping front increases causing it to penetrate farther into the material. This increases both the mobile and trapping inventories. Some new R&D results from laboratory experiments [9] are becoming available and they seem to indicate for Be a much higher recombination coefficient than that assumed for this study and cited in [8] which is probably representative of a situation where carbon could have largely contaminated the beryllium surfaces. As far as the effect of the trap density is concerned, an increase of the density of a factor of 10 more than the base value indicated in Table 2 was found to have strong consequences. Even though at this time there is only preliminary information available, there is no evidence that this very high trap density will exist. R&D is planned in this area.

Finally, the extent of the coverage of blocking layers and its stability with off-normal thermal transients is difficult to estimate at this point. The inventory reduction could be substantial if these areas are a significant fraction of the first wall and low-flux divertor regions.

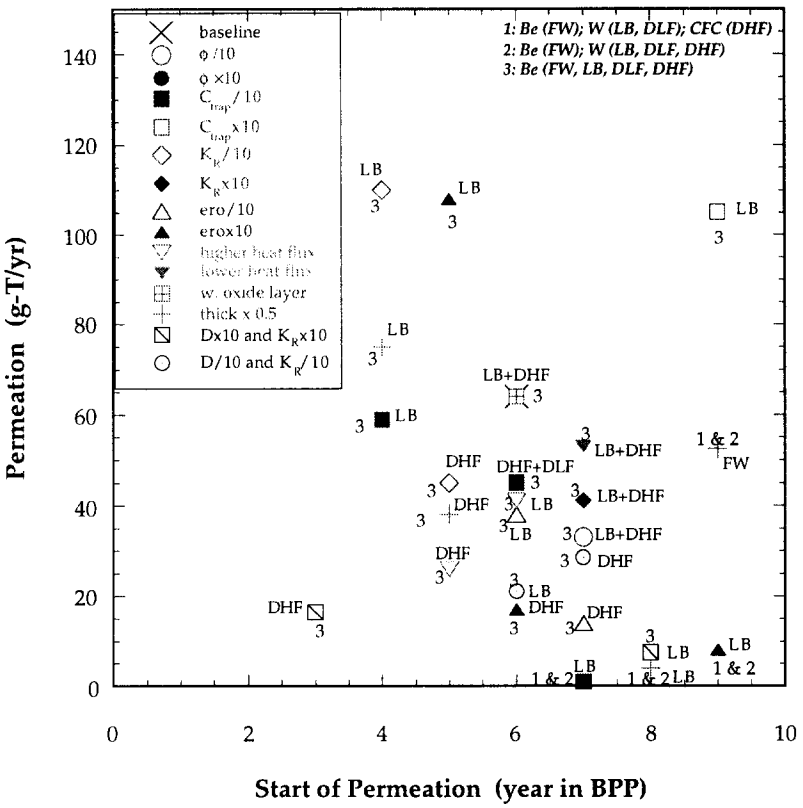


Fig. 3. Yearly permeation rate versus the starting time of permeation measured in years into the BPP. Numbers in the figure refer to the various design options analysed. (Abbreviations: FW = first wall, LB = lower baffle, DLF = low flux portion of divertor, DHF = high flux portion of divertor.)

### 4.2. Tritium permeation

In Fig. 3 the yearly permeation rate is plotted against the starting time of permeation measured in years into the BPP and based on the operating history. Note that for case 1 and 2, the use of tungsten and CFC in areas of high heat flux essentially eliminated permeation in the ITER lifetime. Permeation is significant only when beryllium is used to clad high heat flux components exposed to high erosion rates (i.e., the baffle and the divertor). In this case, permeation starts in year 6 at a rate of about 60 g T/yr for the last four years of the BPP. The variations of the parameters which have the strongest implications on the results are: (i) reduction in recombination coefficient; (ii) increase of the diffusion rate; (iii) reduction of the trap density; and (iv) increase in the erosion rate.

Particularly a low recombination coefficient results in higher surface concentration and concentration gradient. This increases the flow into traps at the trapping front, speeds the movement of the front, and results in earlier breakthrough. It also results in higher permeation once breakthrough occurs. The higher diffusion causes more rapid flow of diffusing tritium towards the trapping. As a result, the trapping front moves more quickly. However, the corresponding increase in the surface recombination largely offsets this by reducing the surface concentration that drives the diffusion into the bulk. The net result is some reduction to the breakthrough time. Reducing the trap density speeds up the motion of the trapping front which decreases the time to breakthrough. Erosion reduces the thickness of the material. This both reduces the breakthrough time but also increase the permeation after breakthrough.

## 5. Research and development needs

R&D activity is in progress in the four ITER Home-Teams and priority research items are:

(1) Improve understanding of tritium uptake and release mechanisms in beryllium and measurement of surface recombination coefficient and its dependence on surface purity, surface temperature and particle flux.

(2) The degree of codeposition of T with pure Be or in the presence of other impurities (mainly C and O).

(3) Removal of T-codeposited layers, including investigations on the adhesion and possible flaking, release of tritium as a function of temperature from thick layers.

(4) Effects of neutron induced traps on tritium retention and migration in beryllium, tungsten and CFC's.

(5) Actual measurements of inventory and permeation through duplex structures simulating PFC's, consisting of an amour material joined to a heat sink reproducing correct temperatures and thermal gradients, particle fluxes, presence of interface joint materials between amour and heat-sink.

## 6. Summary

A systematic approach was followed to select parameters with large uncertainty and with a potential for impact on the inventory or permeation. Inventory and permeation was determined for the ranges of these parameters. Based on these results, upper and lower bounds were determined that bracketed most results. As far as the tritium inventory is concerned, for the reference case (i.e., beryllium on the first wall, start-up limiter, upper baffle, tungsten on the lower portion of the baffle and on the low heat flux divertor areas of the divertor, and CFC on the high heat flux area of the divertor) the total mobile inventory is found to be between about 1050 g and 2200 g while the trapped inventory could vary between 530 g and 2400 g T. This assumes accumulations up to 1000 g T of codeposition inventory with subsequent clean-up intervention. Results of the other cases obtained by varying one at the time the various parameters analyzed to cover the ranges of greater uncertainty, are plotted in Fig. 2. As far as tritium permeation is concerned, earliest breakthrough occurs for the lower portion of the baffle when protected by beryllium. For the baseline case, permeation starts during year 6 and reaches 60 g T/yr. Finally, some of the most crucial issues which require additional effort were identified and discussed.

## Acknowledgements

This paper was prepared as an account of work performed under the Agreement among the European Atomic Energy Community, the Government of Japan, the Government of the Russian Federation, and the Government of the United States of America on Co-operation in the Engineering Design Activities for the International Thermonuclear Experimental Reactor ('ITER EDA Agreement') under the auspices of the International Atomic Energy Agency (IAEA).

## References

[1] G. Federici, D.F. Holland, J. Brooks, R. Causey, T. Dolan and G. Longhurst, Proc. 16th IEEE/SOFE, Symp. on Fusion Engineering, Champaign, IL, USA, 30 Sept.–5 Oct., Vol. I (1995) 418–423.

[2] G. Federici, D. Holland and B. Esser, J. Nucl. Mater. 227 (1996) 170–185.

[3] G. Federici, D. Holland and R. Matera, J. Nucl. Mater. 233–237 (1996) 741.

[4] G. Federici and D. Holland, Parameter Study for Tritium Inventory and Permeation in ITER Plasma Facing Components, ITER Report, G 17 RI 15-95-12-13 W 1.2, January (1996).

[5] J. Brooks, R. Causey, G. Federici and D. Ruzic, these Proceedings, p. 294.
[6] W. Eckstein and H. Verbeek, Special Issue in Nucl. Fusion —Data Compendium for Plasma Surf. Int. (1984) 12–28.
[7] Y. Igitkhanov, H.D. Pacher, G. Federici, G. Janeschitz, D.E. Post and I. Smid, 1995 Eur. Physical Soc. on Controlled Fusion and Plasma Physics-EPS Meeting, Bournemouth, UK, July 3–7, Proceedings IV (1995) 333–336.
[8] P.L. Andrew, A.T. Peacock and M.A. Pick, J. Nucl. Mater. 196–198 (1992) 997–1001.
[9] R.A. Causey, G. Longhurst and W. Harbin, these Proceedings, p. 1041.
[10] G. Saibene, R. Sartori, A. Tanga, A. Peacock, M. Pick and P. Gaze, J. Nucl. Mater. 176–177 (1990) 618–623.
[11] Design Description Document, ITER Doc. January (1996).